CrossMark

ORIGINAL ARTICLE

The Use of Cooling Rate to Engineer the Microstructure and Oil Binding Capacity of Wax Crystal Networks

Alexia I. Blake[1] · Alejandro G. Marangoni[1]

Abstract The effects of cooling rate during melt crystallization of rice bran wax, sunflower wax, candelilla wax and a commercial peanut butter stabilizer in peanut oil were evaluated and correlated to their oil binding capacity. Rapid cooling upon crystallization decreased crystal length, decreased network pore area fraction, increased the fractal dimension of the crystal network, and lead to an increase in the oil binding capacity. Oleogels structured using 1 % sunflower wax exhibited the highest oil binding capacity, followed by candelilla wax and rice bran wax gels. The oil binding capacity of the commercial stabilizer was the lowest, but could be improved by crystallizing the material under high cooling rates. Linear correlation analysis revealed that the network fractal dimension decreases as pore area fraction increases, which was correlated to a greater oil loss. In general, the oil binding capacity of a gel can be significantly improved if the pore area fraction is decreased below 96 %, demonstrating how the fractal dimension and pore area fraction of a gel network can be modulated to tailor oil binding capacity.

Keywords Oil binding · Microstructure · Wax · Oleogel · Fractal dimension · Cooling rate

Introduction

The rheological behavior and macroscopic functionality of an oleogel can be tailored by modifying the microstructure of the network [1]. For instance, crystal size, shape and distribution, the degree of branching, and the proportion of transient and permanent junction zones will determine the elasticity, mechanical strength, and oil binding capacity of the gel in question.

These network characteristics can be modulated by external forces such as shear and cooling rate since they affect nucleation and crystallization kinetics. With respect to cooling rate, faster cooling effectively corresponds to a higher time-dependent undercooling or supersaturation [2, 3]. This induces faster rates of nucleation, resulting in more crystallographic mismatches and branching, particularly for fibrillar networks such as those of self-assembled fibrillar networks (SAFINS) [4]. This yields a spherulitic network with a high population of small crystals. Conversely, slower cooling rates can be used to obtain a fibrillar morphology characterized by larger and less-branched crystals. Neighboring fibers interact predominantly at transient junction zones, which are known to provide greater elasticity to a network, while spherulitic and highly branched crystals interact at permanent junction zones, creating a strong network resistant to strain [1].

The correlation between microstructure and macroscopic functionality has been studied for some oleogel systems, including monoglycerides [5, 6] and 12-hydroxystearic acid [2, 7, 8]. These studies have demonstrated the profound impact of network morphology on the rheological behaviour and oil binding capacity of oleogels, emphasizing the importance of understanding the nucleation and crystallization processes and their sensitivity to variables such as cooling rate and shear. With this knowledge, these external variables can be used to modify the microstructure of gel networks to create oleogels with tailored functional properties.

With regards to wax oleogels, Toro-Vazquez et al. have made significant progress in this area. Through several studies, their group has determined that the minor alkane

✉ Alejandro G. Marangoni
amarango@uoguelph.ca

[1] Department of Food Science, University of Guelph, Guelph, 50 Stone Rd East, Guelph, ON N1G2W1, Canada

components present in candelilla wax (CLX) co-crystallize with the major wax component, hentriacontane, during cooling [9, 10]. This co-crystallization results in the formation of rotator phases. Co-crystallization of minor components with major components lowers the three-dimensional crystalline order of these rotator phases and inhibits crystal growth, which is why CLX crystals are smaller and less soluble in oil compared to pure alkanes, as indicated by enthalpy of melting (ΔH_m) values obtained by differential scanning calorimetry [10]. CLX gels also exhibited a higher elastic modulus (G') than pure alkane oleogels. This observation was attributed to the higher solid phase content and smaller crystal size of CLX gels.

These authors also concluded that faster cooling rates reduced the efficiency of molecular packing in the solid state, further reducing crystal size and the level of molecular organization of the rotator phases. As a result of this microstructural change, CLX gels that were rapidly cooled exhibited lower G' values compared to slowly cooled gels.

In a separate study, Hwang et al. examined the effect of cooling rate on the texture and firmness of sunflower wax (SFX) oleogels [11]. As expected, they observed a decrease in crystal size with increasing cooling rate. These authors also commented on the effects of cooling rate on crystal shape. Slower cooling allowed for the growth of larger and consistently shaped crystals, while faster cooling produced incongruently shaped small crystals. It was also reported that faster cooling increased gel firmness. A dense network of small crystals, they concluded, is more effective at resisting deformation compared to a network of larger crystals.

Zulim-Botega et al. examined the effect of cooling rate on rice bran wax (RBX), CLX, and carnauba wax (CRX) oil gelling ability when incorporated into ice cream [12]. Slower cooling rates induce the formation of larger crystal aggregates for RBX, and to large spherulites for CRX. No changes in crystal size were observed for CLX. Changes in crystal size and distribution were shown to effect the fat destabilization process, meltdown resistance, and overrun of ice cream containing waxes. In particular, RBX was found to crystallize at the edge of oil droplets, providing a level of fat stabilization and structuring comparable to saturated fat, allowing for a substitution of saturated fat with wax.

These works highlight the influence of cooling rate on the morphology and size of wax crystals. Given that network structure is strongly correlated to macroscopic properties such as elasticity, mechanical strength, and oil binding capacity, it is important to understand how to manipulate nucleation and crystallization processes to intentionally obtain specific morphologies with predictable functionality.

For wax oleogels, such work is still in its infancy, as the focus of most work has been on the characterization of plant-based wax oleogels under static conditions and with no regard for their oil binding capacity. This is of concern for two reasons. First, studying oleogels under static conditions does not provide any indication of how these gels will behave when exposed to industrial processing conditions that utilize shear, agitation, and variable cooling. Secondly, the oil binding capacity of an oleogel is perhaps its most important measure of functionality since it will dictate which applications may benefit from oil gelation.

For instance, oleogels have been considered as fat replacements for meat products [13]. An oleogel with a low oil binding capacity would easily exude oil into the surrounding food matrix upon chewing, altering the textural and sensory properties of the product in an undesirable manner. If the oil binding capacity of the gel could be improved by manipulating the gel microstructure, perhaps by altering processing conditions (i.e., cooling rate), then the use of oleogels as fat replacement could be realized. In short, oleogel behavior when exposed to industrial processing conditions must be considered in order to properly assess the potential use of oleogels as fat replacements, and more generally as oil binding materials.

In a previous study, we assessed the oil binding capacity of RBX, SFX, CLX, and CRX gels, and found that CLX gels retained the most oil [14]. We attributed this to the morphology of the wax, which has recently been identified as platelet-like in nature [15]. We hypothesized that the small crystals present in CLX networks provide more surface area for oil to adsorb onto compared to the larger crystals found in RBX, SFX, and CRX oleogels.

In the same study, we discussed the contributions of tightly bound oil and loosely bound oil to overall oil binding capacity. This not only raises questions about entrapment and adsorption as oil binding mechanisms, but also suggests that there may be a difference between "oil structuring" and "oil binding". The former may refer to gelation processes that sequester the oil and prevent liquid flow, while the latter expresses the strength and nature of the interactions between gelator and solvent, particularly when the gel is mechanically stressed. However, further work is required to understand which attributes of a gelator are required to achieve both gelation and strong oil binding.

This study aims to fill this gap by examining the effect of cooling rate on the oil binding capacity of three wax oleogels. Changes in network morphology including crystal length, fractal dimension, and pore area, are used to explain oil loss trends in an attempt to elucidate the contribution of entrapment and adsorption on oil binding capacity. The oil binding capacity of wax oleogels are compared to those of oleogels prepared with an industrial commercial stabilizer to further

emphasize the remarkable oil structuring ability of plant-based waxes.

Materials and Methods

Gel Preparation

Gels were prepared by depositing a known amount of solid wax or commercial stabilizer in a 15 mL glass vial containing peanut oil. The wax-oil mix was placed in a 90 °C oven for 30 min to allow for complete melting and dissolution of wax crystals. After melting, the molten gel was distributed among 1.5 mL plastic centrifuge vials (three vials per gel). Vials were cooled under quiescent conditions (23 °C) for 24 h before testing.

Wax concentrations included 0.5 , 1 , 2 , and 5 % (w/w), and concentrations of the commercial stabilizer included 5 , 6 , 7 , and 8 % (w/w). These concentrations were selected to include wax concentrations that were below, equivalent to, and above the critical concentration of each gelator, denoted as C_g. The C_g of the commercial stabilizer was 6.5 % (w/w), while that of RBX, SFX, and CLX were determined to be 1 , 1 , and 2 % (w/w), respectively. This values are in agreement with previous reports, and were determined using an inversion test, as described in our previous study [14]. Waxes were provided by Koster Keunan Inc., (Connecticut, USA) and the commercial stabilizer by Danisco, Grindsted PS105 K-A. The stabilizer, typically added to peanut butter to prevent oil separation, is a blend of fully hydrogenated rapeseed, soybean, and cottonseed oils [16]. The major fatty acids present in the stabilizer are stearic acid (57 %), behenic acid (25 %), palmitic acid (11 %), and arachidic acid (5 %).

Critical Concentration

In this study, the critical gelation concentration, denoted as C_g, has been defined as the minimum amount of wax required to gel liquid oil. This value was determined by preparing 10 g of wax oleogels with decreasing concentrations of waxes in cylindrical 20-mL scintillation vials. The molten wax oleogel was cooled under ambient temperatures (23 °C) prior to testing. The testing procedure was also conducted at the same temperature, and involved inverting the containers. The concentration at which there was no visually-observable flow within the vial was taken as the C_g.

Crystallization at Different Cooling Rates

Statically cooled samples were cooled at 1.5 °C/min or 5 °C/min. A cooling rate of 1.5 °C/min was achieved by cooling against air at room temperature, while cooling at 5 °C/min was achieved using a series of water baths calibrated to different temperatures. The cooling process for 5 °C/min gels was as follows. First, molten gels were distributed among 1.5 mL plastic centrifuge vials (three vials per gel) and placed in a 72 °C water bath for 15 min to melt the waxes. The vials were then placed in a 64 °C water bath for 60 s, placed at room temperature (23 °C) for 60 s, placed in a 55 °C water bath for 60 s, placed at room temperature for four minutes, and then placed in a 10 °C incubator for three minutes until the gels reached a temperature of 23 °C, as determined using a thermometer probe. Once gels reached this final temperature, they were kept under quiescent conditions for 24 h before further testing. Temperature was monitored using a digital thermometer. The variance in cooling rate was ±0.5 °C/min.

To compensate for inconsistencies in cooling rate due to heat loss while transferring gels between water baths, batches containing gels of equivalent wax concentrations were cooled simultaneously. For instance, all 1 % gels were cooled in the same batch so that oil loss results were comparable given that all waxes were exposed to the same cooling process.

Brightfield Microscopy

Samples were prepared by depositing a drop of gel onto a heated glass microscope slide. The gel was pressed with a glass cover slip to ensure a sample thin enough for light microscopy. Slides were allowed to cool under quiescent conditions for 24 h before imaging. Slides were prepared in triplicate, and micrographs were obtained using a 40× objective lens. Imaging was conducted at ambient temperatures using a Leica DM RXA2 microscope in brightfield mode (Leica Microsystems, Richmond Hill, Canada) equipped with a CCD camera (Q Imaging Retiga 1300, Burnaby, BC, Canada). Images were acquired using Openlab 6.5.0 software (Improvision, Waltham, MA, USA) and a 40× objective lens (Leica, Germany). Images were obtained in triplicate.

Oil-Binding Capacity

The oil-binding capacity was measured by centrifuging a 1.5 mL plastic centrifuge vial containing a known mass of sample (approximately 1–1.5 g) for 30 min in an Eppendorf Centrifuge 5410, at its maximum rotary speed of 14,000 rpm (relative centrifugal force=21.8×10³ g). Centrifuge vials were weighed before and after the addition of gels so that the actual sample mass could be obtained. After each centrifugation cycle, the released oil at the surface was decanted, and the mass of the sample was determined. This was repeated for four centrifuge cycles, with

each cycle lasting 30 min. OL_1 and OL_4 denote oil loss after the first and final centrifugation cycles, respectively.

These values were calculated as the percentage of decanted oil after the first and final centrifuge cycle:

$$\text{Oil-Loss after cycle}_i\ (OL_i) = \frac{\text{Initial Sample Mass} - \text{Sample Mass after Decanting after cycle}_i}{\text{Initial Amount of Oil in Sample}} \times 100\%$$

Oil-loss values for each gel were calculated as the mean of three replicates, with standard errors for each calculated value. Oil lost during the first centrifuge cycle (OL_1) is considered to be weakly bound oil that is entrapped within the scaffolding of the network. Thus, a high OL_1 value suggests that the network contains a significant proportion of weakly bound oil, and that the short-term oil binding capacity of the network is low. In comparison, OL_4 is representative of long-term oil binding. A low OL_4 value means that much of the oil present in the network is tightly bound. Therefore, the long-term oil binding capacity of the network is high.

Microstructural Analysis

ImageJ (National Institute of Mental Health, Bethesda, ML, USA) was used to measure crystal length from the micrographs. The measuring tool in the software program was calibrated using the scale bar of each micrograph. A line was then drawn along each crystal, and the length of that line was recorded as the crystal length. Results are reported as the mean and standard error of three micrographs.

Fractal Dimension and Pore Area Fraction

The box-counting fractal dimension of micrographs was determined using Benoit 1.3 (Trusoft International Inc., St. Petersburg, FL, USA). Micrographs were thresholded using Adobe Photoshop CS2 (Adobe Systems Inc., San Jose, USA) using the automatic threshold setting, and processed by Benoit 1.3 (Trusoft International Inc, St. Petersburg, FL, USA) to give a box-counting fractal dimension (http://www.trusoft-international.com/benoit.html). The fractal dimension reported here is an average taken from three micrographs. The box-counting fractal dimension, denoted as D_b, is a numerical indication of the homogeneity of mass distribution. For two-dimensional images, the closer the D_b is to 2, the more evenly distributed the mass within that network. In comparison, a lower D_b is associated with less evenly distributed (or clustered) mass.

The percentage of white pixels in each micrograph is indicative of solid crystalline material, and is reported as the % Fill. The remaining black pixels correspond to the pores.

Thus, the percentage or pore area fraction, AF_p, can be determined using the following relationship:

$$AF_p = 1 - \frac{\%Fill}{100}$$

As the percentage of black pixels present in a micrograph increases, so does the pore area fraction.

Statistical Analysis

GraphPad Prism 5.0 (GraphPad Software, San Diego, CA, USA) was used for curve-fitting and statistical analysis. Two-way analysis of variance (ANOVA) and linear correlations between the microstructural data and oil-binding parameters of gels were conducted with three replicates for each measurement for each gel. The level of significance for a correlation was chosen as $p < 0.05$. Graphical figures were exported from Graphpad Prism 5.0 as tiff files.

Results and Discussion

In a previous study, we measured the oil binding capacity of wax oleogels in canola oil at their gelation concentration, C_g [14]. The oil present in the material was considered to be either weakly-bound oil that is entrapped within the pores, or tightly-bound oil that is adsorbed onto the surfaces of the wax crystals. Weakly-bound oil will exude from the system over a shorter period of time compared to tightly-bound oil, which may not even exude over the time scale of the experiment. A high proportion of weakly-bound oil is expected to result in more oil loss. Thus, by decreasing the amount of weakly-bound oil (or increasing the amount of tightly-bound oil), the oil binding capacity of the network will increase.

In our study, we found that as the solid mass is more evenly distributed throughout the material, the oil present in the material becomes more strongly bound [14]. One explanation is that such a network will contain a higher number of smaller crystals compared to a network comprised of clustered mass. Thus, a network of evenly distributed crystals will provide more surface area for adsorption compared to one of larger crystal clusters, increasing the amount of oil that is tightly bound by increasing the amount of surface that the oil can

adsorb onto. This reduces the amount of fast-leaking or weakly-bound oil, resulting in less oil loss.

Similar correlations were conducted in this study to improve our understanding of the relationship between gel microstructure and oil binding capacity. More specifically, linear correlation analysis between microstructural parameters (D_b, AF_p, wax concentration) and oil loss values (OL_1 and OL_4) were conducted for all concentrations of RBX, SFX, and CLX gels. These results are summarized in Tables 1 and 2.

As seen in Tables 1 and 2, OL_1 and OL_4 correlate negatively with D_b. As previously explained, this is likely due to the increase in surface area for oil adsorption achieved by evenly distributing the mass. Thus, a network of homogeneously distributed mass will contain a relatively larger amount of tightly bound oil, and therefore will exhibit less oil loss.

D_b was also shown to negatively correlate with AF_p, while AF_p correlated positively with oil loss. What these correlations suggest is that a network comprised of clustered mass will contain larger pores and exhibit more oil loss compared to a network of evenly distributed mass and smaller pores. Not only will the latter network contain a larger proportion of tightly bound (adsorbed) oil, but the weakly bound oil will have to migrate through a highly tortuous network in order to exude.

From a structural perspective, these findings indicate that the oil binding capacity of a gel can be improved by increasing the homogeneity (or order) in the distribution of crystal mass (D_b), or decreasing pore area fraction (AF_p). In this study, we examined how cooling rate and wax concentration affect these two microstructural parameters. The former is a direct manipulation of the gel microstructure, while the latter option is simply a means of increasing the solid volume fraction of the gel. This reduces the total liquid volume and also provides more "structuring" material to support the network.

The relationships between D_b, AF_p, and oil loss was explored further given the compelling evidence suggesting that these microstructural parameters can be used to attenuate oil loss. D_b was plotted against AF_p for all oleogels exposed to both cooling conditions. The resulting curve, shown in Fig. 1,

Table 2 Linear correlation analysis of structural parameters and oil loss data for wax gels cooled at 5 °C/min

5 °C/min	D_b	OL_1	OL_4	AF_p	% Wax
D_b	–	-0.88^b	-0.95^c	-0.90^c	0.63^a
OL_1	-0.88^b	–	0.93^c	0.74^b	
OL_4	-0.95^c	0.93^c	–	0.80^b	-0.66^a
AF_p	-0.90^c	0.74^b	0.80^b	–	-0.64^a
% Wax	0.63^a		-0.66^a	-0.64^a	–

The level of significance is denoted by superscript letters a ($p<0.05$), b ($p<0.01$), and c ($p<0.0001$)

can be modeled using an exponential function of the following form $D_b = A + Be^{-AF_p/C}$, where A, B, and C are fitting parameters.

The significance of this finding is that D_b is strongly related to AF_p. This means that the total pore area of a system can be manipulated to achieve a specific D_b, irrespective of wax type or cooling rate. Given that oil loss has been found to correlate with D_b, this presents an extremely powerful means of engineering the oil binding capacity of wax oleogels.

Oil loss can also be plotted as a function of pore area fraction, as shown in Fig. 2. This relationship can be modeled using a simple exponential growth function. Again, because this relationship applies to oleogels containing different concentrations of three unique wax species cooled under two different cooling rates, this finding demonstrates how, as a general rule, the pore area can be modified to tailor the oil binding capacity of wax oleogels.

This figure also reveals that there is a pore area threshold below which the oil binding capacity is greatly diminished. By performing a linear regression on the region containing increasing oil loss values of the figure above, this threshold (taken as the x-intercept) was determined to be 96.8 % ($R^2 = 0.99$). This finding suggests that the oil binding capacity of a network can be improved by reducing the pore area fraction to below 96 %. One means of achieving this modification is by increasing wax concentration. An alternative is by applying a higher cooling rate during gel preparation.
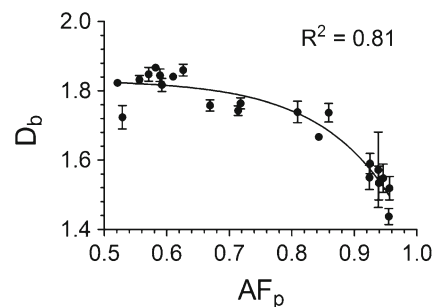
Table 1 Linear correlation analysis of structural parameters and oil loss data for wax gels cooled at 1.5 °C/min

1.5 °C/min	D_b	OL_1	OL_4	AF_p	% Wax
D_b	–	-0.79^b	-0.85^b	-0.94^c	0.79^b
OL_1	-0.79^b	–	0.82^c	0.66^a	-0.59^a
OL_4	-0.85^b	0.82^c	–	0.86^b	-0.80^b
AF_p	-0.94^c	0.66^a	0.86^b	–	-0.91^c
% Wax	0.79^b	-0.59^a	-0.80^b	-0.91^c	–

The level of significance is denoted by superscript letters a ($p<0.05$), b ($p<0.01$), and c ($p<0.0001$)

Fig. 1 Fractal dimension (D_b) as a function of pore area fraction (AF_p) for rice bran wax (RBX), sunflower wax (SFX), and candelilla wax (CLX) gels cooled at both 1.5 °C/min and 5 °C/min
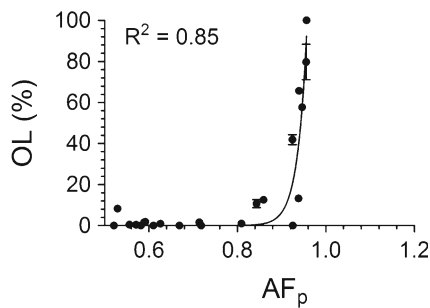
Fig. 2 Oil loss (OL) as a function of pore area fraction (AF_p) for rice bran wax (RBX), sunflower wax (SFX), and candelilla wax (CLX) gels cooled at both 1.5 °C/min and 5 °C/min

Armed with this knowledge, differences in oil loss values were interpreted by examining how factors such as cooling rate, wax type, and wax concentration impact the microstructural characteristics of the wax crystal network, namely D_b, AF_p, and mean crystal length. A commercial stabilizer (CS) commonly added to peanut butter to prevent oil separation was included in this study. The C_g of the CS is 6.5 % (w/w), which is noticeably higher than that of RBX, SFX, and CLX. The difference in C_g between these gelators demonstrates the superior oil structuring ability of waxes relative to commercial stabilizers.

Unfortunately, CS oleogels were too dense to image using optical light microscopy due to the high solid concentrations required for gelation. As a result, it was not possible to obtain any information about crystal length, D_b, or AF_p. Only the OL_1 and OL_4 values of CS oleogels can be compared to the OL_1 and OL_4 values of wax oleogels. OL values are listed in Table 3.

Oil Loss Results – Slow Cooling vs. Fast Cooling

As seen in Table 3, rapidly cooled 1 and 2 % RBX gels exhibited lower OL_1 and OL_4 compared to slowly cooled RBX gels at equivalent wax concentrations ($p<0.05$). Rapidly cooled 1 and 2 % gels had higher fractal dimensions, D_b, ($p<0.0001$) and smaller pore area fraction, AF_p ($p<0.001$), shown in Tables 4 and 5. At equivalent wax concentrations, the mean crystal length decreased when gels were rapidly cooled ($p<0.0001$). Mean crystal lengths are listed in Table 4.

From a structural perspective, this means that faster cooling created a network of homogeneously distributed small crystals. As previously explained, the even distribution of crystalline mass provides more surface area and reduces pore area fraction (AF_p), creating a highly tortuous pathway for loose oil to migrate through before escaping the network [14]. As a result, there is less oil loss compared to slowly cooled gels which contain clustered crystals and larger pores, allowing larger volumes of oil to migrate through a less tortuous network.

The difference in D_b, or AF_p was not statistically significant for 5 % RBX gels. As expected, there was also no significant difference in oil loss values for 5 % gels either. The 0.5 % gels lost more oil when cooled rapidly ($p<0.05$). There was no difference in D_b or AF_p between rapidly cooled or slowly cooled 0.5 % gels, which explains this observation. However, as shown in Table 6, slowly cooled 0.5 % gels contained longer crystals compared to 0.5 % rapidly cooled RBX gels ($p<0.0001$). It is possible that at such low wax concentrations, longer crystals are more efficient at structuring large volumes of oil by entrapping it within the wax crystal scaffolding.

Table 3 Oil loss values after the first centrifuge cycle (OL_1) and last centrifuge cycle (OL_4) for wax gels cooled at 1.5 °C/min and 5 °C/min. Means with same superscript are not significantly different ($p>0.05$)

	Slow Cooling (1.5 °C/min)				Rapid Cooling (5 °C/min)			
0.5 %	RBX	SFX	CLX	5 % CS	RBX	SFX	CLX	5 % CS
OL_1	65.69±2.07[a]	Gel did not form	Gel did not form	51.56±0.52[h]	79.7±14.87[j]	41.86±4.15[l]	Gel did not form	33.9±1.96[n]
OL_4	78.44±3.88[a]			60.73±0.28[hij]	90.16±8.23[l]	74.18±2.16[l]		47.3±1.81[q]
1 %	RBX	SFX	CLX	6 % CS	RBX	SFX	CLX	6 % CS
OL_1	57.66±0.99[b]	0[e]	12.59±2.19[f]	55.27±2.67[b]	0[k]	8.29±1.64[m]	13.24±0.98[fm]	31.3±1.96[no]
OL_4	78.25±4.41[a]	49.7±10.15[d]	80.92±0.6[a]	62.48±2.35[i]	62.38±0.83[m]	34.43±5.05[p]	44.32±8.49[op]	43.4±1.83[o]
2 %	RBX	SFX	CLX	7 % CS	RBX	SFX	CLX	7 % CS
OL_1	10.68±3.35[c]	1±1.25[ek]	0.88±0.31[eg]	49.41±1.49[h]	1.54±1.24[ck]	1.62±0.39[ek]	0.42±0.26[k]	28.33±1.41[op]
OL_4	34.67[b]	9.46±3.07[eq]	8.07±4.22[ef]	58.4±0.79[j]	4.59±0.41[n]	12.28±0.85[q]	2.15±0.97[p]	39.76±2.74[s]
5 %	RBX	SFX	CLX	8 % CS	RBX	SFX	CLX	8 % CS
OL_1	1.83±0.22[d]	0.49±0.33[de]	0[e]	38.22±1.74[i]	0[dk]	0[ek]	0[ek]	26.8±0.43[p]
OL_4	16.68±6.16[c]	2.59±1.09[er]	0.52±0.22[g]	49.31±1.68[k]	0.52±0.15[n]	0.34±0.29[nr]	0.32±0.04[gnp]	38.86±0.74[s]

OL_1 means were not compared with OL_4 means. Slowly cooled gels were compared to rapidly cooled gels containing equivalent concentrations of the same wax species, and to slowly cooled gels containing different concentrations of the same wax species and equivalent concentrations of different wax species. Rapidly cooled gels were also compared to rapidly cooled gels containing different concentrations of the same wax species and equivalent concentrations of different wax species. Reported values are averages and standard errors of three replications

Table 4 Fractal dimensions (D_b) for gels cooled at 1.5 °C/min and 5 °C/min. Means with the same superscript are not statistically different ($p > 0.05$)

D_b		0.5 %	1 %	2 %	5 %
RBX	1.5 °C/min	1.53±0.049[a]	1.55±0.041[a]	1.67±0.005[b]	1.82±0.019[c]
SFX		1.52±0.034[ad]	1.52±0.029[a]	1.74±0.031[bd]	1.83±0.012[bc]
CLX		–	1.74±0.027[e]	1.86±0.017[ef]	1.84±0.009[cef]
RBX	5 °C/min	1.44±0.023[a]	1.76±0.016[c]	1.85±0.018[cf]	1.82±0.002[cf]
SFX		1.55±0.035[d]	1.72±0.034[cd]	1.74±0.014[d]	1.76±0.016[cd]
CLX		–	1.57±0.109[c]	1.85±0.02[df]	1.87±0.009[df]

D_b values were compared between gels containing equivalent concentrations of different wax species cooled under the same cooling rate, and between gels containing different concentrations of the same wax species cooled under different cooling rates. Reported values are averages and standard errors of three replications

Not surprisingly, the mean crystal length was smaller for rapidly cooled SFX gels compared to slowly cooled SFX gels at equivalent concentrations ($p < 0.0001$). Differences in oil loss between slowly cooled and rapidly cooled gels were statistically different between 1 % SFX gels only. The 1 % rapidly cooled gels had lower OL_4 ($p < 0.0001$) compared to slowly cooled 1 % gels, but a higher OL_1 ($p < 0.05$). Rapidly cooled 1 % SFX gels also had a higher D_b ($p < 0.01$) and smaller AF_p ($p < 0.01$) compared to slowly cooled 1 % gels.

Again, these structural differences imply that faster cooling results in a homogenous distribution of smaller crystals, as indicated by a high D_b and low AF_p. The final network contains a large amount of surface area and small amount of pore space. As crystalline surface area increases, so does the amount of adsorbed oil. If adsorbed oil is considered to be tightly bound oil, then an increase in crystal surface area would result in an increase in the amount of tightly bound oil. This would cause a decrease in the percentage of exuded oil from the network, explaining why rapidly cooled 1 % SFX gels had lower OL_4 values compared to slowly cooled 1 % SFX gels.

The 0.5 % SFX gels formed only under high cooling rates. There were no statistical differences between D_b or AF_p between slowly cooled and rapidly cooled 0.5 % SFX gels. The only observable difference was that rapidly cooled 0.5 % SFX gels contained shorter crystals than slowly cooled 0.5 % SFX

gels ($p < 0.0001$). Although this morphological difference is expected, it is not in agreement with the trends observed for 0.5 % RBX gels, which experienced less oil loss when exposed to slower cooling rates. At 0.5 % wax concentration, longer crystals appeared to be more efficient at structuring oil for RBX, while the opposite is true for 0.5 % SFX gels.

This might be a consequence of surface effects. The chemical composition and topographical features of the exposed wax crystal surface will influence the degree of interaction with the surrounding liquid medium. The "wettability" of a surface is one manifestation of this relationship. The spreading parameter (S) is an indication of the 'wettability' of a surface [17]. It describes how a liquid droplet interacts with a solid interface based on the surface energy (γ) of the solid, $S = \gamma_{solid} - (\gamma_{liquid} + \gamma_{solid-liquid})$. Total wetting is achieved when the droplet completely spreads over the surface, yielding $S > 0$. As seen from the equation above, this requires γ_{solid} to be large. In the case of partial wetting, the droplet does not spread over the surface, but instead forms a round bead, minimizing the area of contact with the solid. This scenario results in $S < 0$.

The wettability of a surface is also dependent on the compatibility between the solid surface and liquid droplet, determined by the chemical nature of the two interfaces. For instance, if the chemical nature of a wax crystal is highly compatible with the surrounding oil phase, then oil will easily adsorb onto the crystal surface, yielding $S > 0$. If the chemical

Table 5 AF_p for gels cooled at 1.5 °C/min and 5 °C/min. Means with the same superscript are not statistically different ($p > 0.05$)

AF_p		0.5 %	1 %	2 %	5 %
RBX	1.5 °C/min	0.94±0.013[a]	0.95±0.006[a]	0.84±0.007[b]	0.59±0.036[c]
SFX		0.96±0.007[a]	0.93±0.016[ae]	0.81±0.037[b]	0.56±0.04[c]
CLX		–	0.86±0.01[e]	0.63±0.016[c]	0.61±0.029[c]
RBX	5 °C/min	0.96±0.005[a]	0.72±0.011[b]	0.59±0.023[c]	0.52±0.034[c]
SFX		0.9±0.019[a]	0.69±0.019[b]	0.71±0.021[bd]	0.62±0.012[d]
CLX		–	0.94±0.001[e]	0.57±0.038[c]	0.549±0.039[c]

AF_p values were compared between gels containing equivalent concentrations of different wax species cooled under the same cooling rate, and between gels containing different concentrations of the same wax species cooled under different cooling rates. Reported values are averages and standard errors of three replications

Table 6 Mean crystal lengths (μm) for wax oleogels cooled at two different cooling rates

% Wax	RBX - 1.5 °C/min		RBX - 5 °C/min		SFX - 1.5 °C/min		SFX - 5 °C/min		CLX - 1.5 °C/min		CLX - 5 °C/min	
	Mean (μm)	S.E.M	Mean (μm)	S.E.M	Mean (μm)	S.E.M	Mean (μm)	S.E.M	Mean (μm)	S.E.M	Mean (μm)	S.E.M
0.5	15.3[a]	0.36	6.23[c]	0.40	12.5[e]	0.27	4.1[g]	0.20	–		–	
1	16.3[a]	0.43	9.71[d]	0.50	16.4[af]	0.31	6.9[h]	0.26	5.2[i]	0.12	3.3[l]	0.06
2	20.8[b]	0.47	10.4[d]	0.47	16.2[f]	0.22	10.8[d]	0.51	5.8[j]	0.12	4.2[m]	0.06
5	21.0[b]	0.44	9.81[d]	0.42	16.4[f]	0.23	11.2[d]	0.46	8.1[k]	0.17	6.1[n]	0.11

Means with the same superscript are not statistically different ($p>0.05$). Mean lengths were compared between gels containing equivalent concentrations of the same wax species cooled under different cooling rates, while gels containing equivalent concentrations of different wax species or different concentrations of the same wax species were compared under the same cooling rate. Reported values are averages and standard errors of three replications

nature of the crystal is less compatible, then less oil will be adsorbed. In the latter case, entrapment may be a more suitable oil binding mechanism, in which case longer crystals would be preferable.

According to wax suppliers Koster Keunan Inc., RBX contains long chain saturated C46-C62 esters, while SFX consists of long chain saturated C42 to C60 esters. Similar chain lengths suggest no difference in hydrophobicity. However, the acid value for RBX is 13, approximately three times more than the acid value of SFX. This suggests that there is a greater presence of carboxylic acid groups in RBX compared to SFX. The double-bonded oxygen and hydroxyl groups within a carboxyl group enhance the hydrophilic nature of a species, hinting at difference in the chemical nature of RBX and SFX. However, further characterization is required to confidently distinguish between such differences.

Another factor to consider is the roughness of the surface [18]. According to the Wenzel equation, increasing the roughness of a hydrophobic surface will increase its wettability when exposed to a hydrophobic medium. The explanation for this is that a rougher surface will have more surface area, allowing for greater contact with the hydrophobic liquid. For a hydrophilic surface, any topological troughs or crevices will be occupied by air, minimizing the interfacial contact area between droplet and solid surface. This condition can be modeled using the Cassie-Baxter equation [18].

Razul et al. examined the effects of surface hardness on oil binding capacity [19]. By using atomic scale molecular dynamics computer simulations to model the nanoscale oil binding capacity between parallel sheets of tristearin crystalline nanoparticles (CNP), the authors determined that oil binding increased when the CNP surfaces were softer. These findings demonstrate how surface texture can be used to attenuate oil binding. This is an important concept and suggests that the nature of the network surface should be considered as another variable contributing to oil binding.

These findings support the proposal that differences in chemical composition and roughness of wax crystal surfaces will lead to differences in oleogel oil binding capacity. If the topological properties of the wax network promote high levels of wetting, then it is likely that the wax will bind oil via adsorption and exhibit a high oil binding capacity. Alternatively, a network with surface conditions that are less favorable for wetting may instead bind oil by entrapment, rather than adsorption.

Thus, the difference observed between 0.5 % RBX and 0.5 % SFX may be due to differences in oil binding mechanisms. RBX oil binding capacity may depend on entrapment for oil binding, while SFX may depend on adsorption, in which case shorter crystals with a greater surface are preferable.

Rapidly cooled CLX gels contained shorter crystals compared to slowly cooled CLX gels at equivalent wax concentrations ($p<0.0001$). Rapidly cooled gels had a lower OL_4 ($p<0.05$), while OL_1 was not statistically different. There was no significant difference in D_b or AF_p between gels of equivalent wax concentrations cooled at different cooling rates. However, a decrease in crystal size due to rapid cooling would mean an increase in wax crystal surface area, providing more area for oil adsorption, thereby increasing the amount of tightly bound oil. OL_4 was lower for rapidly cooled gels because a larger portion of the total bound oil is tightly bound compared to slowly cooled gels, and therefore more difficult to remove.

For CS oleogels, rapid cooling decreased both OL_1 and OL_4 at equivalent gelator concentrations ($p<0.05$). The assumption that this is due to the formation of smaller crystals cannot be proved due to a lack of microscopic data. However, it is a logical assumption given that the relationship between cooling rate (or more specifically, the degree of supercooling and supersaturation of the melt) and crystal size also applies to fat crystal networks [20, 21].

From this analysis, it is clear that rapid cooling decreases crystal size. A network of smaller crystals will have more surface area available for oil adsorption compared to a network of larger crystals. However, the nature of the crystal surface will dictate the extent of surface wetting and oil adsorption, influencing the amount of oil that is tightly bound.

Apart from decreasing crystal size, rapid cooling was found to increase D_b and decrease AF_p. The interpretation of these results is simply that the network contains homogenously distributed crystal mass and small pores. This will reduce oil loss given that the network will contain less weakly bound oil compared to a network containing clustered mass or more pores, meaning that the volume of free oil must migrate through a highly constricted and tortuous pathway, slowing oil movement and reducing oil loss.

It was noted that significant differences in oil loss related to changes in AF_p and D_b occurred more frequently in 1 and 2 % gels, and less commonly in 0.5 and 5 % gels. One possible explanation is that a 5 % wax concentration may impart too much "solid" character to the network, while 0.5 % wax concentrations yielded a liquid-like system. As discussed in our previous paper, a definition of a "gel" that is both clear and applicable to various gelled system is lacking, providing a challenge in distinguishing the boundary between a gel and solid. There may exist a threshold solid concentration above which the solid volume fraction is so high that it dominates the physical behaviour of the system, causing a transition from gel state to solid state. The 5 % concentration may be included in this range, meaning that the oil binding capacity of 5 % gels is not as sensitive to D_b and pore area as "true" gels containing less wax. Similarly, at very low solid concentrations, a 'weak' gel state may develop with unique properties that do not completely align with the behaviour of a 'true' gel.

Oil Loss - Slow Cooling Rates

As seen in Table 3, at equivalent wax concentrations, RBX gels lost more oil than SFX gels ($p < 0.05$). This observation is in agreement with our previous study, in which C_g RBX gels lost more oil than C_g SFX gels [14]. Interestingly, there was no difference in D_b or AF_p between gels containing the same amount of wax. Meanwhile, 2 and 5 % RBX gels had longer crystals than 2 and 5 % SFX gels ($p < 0.001$), and there was no difference in mean crystal length for 1 % gels.

This alludes again to surface effects that could be related to surface chemistry and surface roughness. First, it is possible that functional groups present at the surface of SFX crystals are more non polar in nature than the functional groups present at the surface of RBX crystals. In an oil medium, this would increase the wettability of SFX crystal surfaces, resulting in greater oil adsorption compared to RBX.

RBX gels lost more oil than CLX gels ($p < 0.001$). The 1 and 2 % RBX gels had a lower D_b ($p < 0.001$) and higher AF_p compared to CLX gels of the same concentration ($p < 0.05$). This means that RBX crystal mass was more clustered compared to CLX crystal mass, resulting in a network with larger pores. In addition, RBX crystals were longer compared to CLX crystals ($p < 0.0001$), reducing the total surface area available for adsorption.

The 1 % CLX gels lost more oil than 1 % SFX gels ($p < 0.001$). The D_b was lower for 1 and 2 % SFX gels ($p < 0.05$), and SFX contained longer crystals ($p < 0.001$). The AF_p was not statistically different for 1 % CLX and SFX gels. CLX crystals would have a greater surface area than SFX crystals since they are smaller in size. More oil adsorption would therefore be expected for CLX crystals. However, OL_1 and OL_4 were higher for 1 % CLX gels because the network binds oil via adsorption, and not entrapment. In comparison, SFX can rely on both mechanism, and therefore exudes less oil.

From this comparison, it is clear that under slow cooling conditions, 1 and 2 % SFX oleogels exhibited the highest oil binding capacity. At higher wax concentrations, the oil binding capacity of SFX and CLX oleogels were superior and comparable. The CS retained significantly less oil compared to 2 and 5 % gels, while the difference in oil loss between CS and wax oleogels was less dramatic at 1 and 2 % gelator concentrations. However, the concentration of CS required to achieve gelation is much higher, and does not offer a relatively superior oil binding capacity.

Oil Loss - High Cooling Rate

Rapidly cooled 0.5 % RBX gels lost more oil than 0.5 % SFX gels ($p < 0.0001$). The 0.5 % RBX gels had a lower D_b ($p < 0.05$) and longer crystals compared to 0.5 % SFX gels ($p < 0.01$). A lower D_b implies that the amount of fast leaking/weakly bound oil increases due to a decrease in the amount of tightly bound/slow leaking oil. The 1 % RBX gels lost more oil than 1 % SFX gels ($p < 0.001$). There was no difference in D_b or AF_p for 1 % gels, suggesting that the differences in oil loss are due to surface effects, especially since RBX consistently exhibits a lower oil binding capacity compared to SFX gels.

OL_1 was higher for 1 % CLX gels ($p < 0.01$) compared to 1 % RBX gels, and OL_4 was higher for 1 % RBX ($p < 0.001$). There was no difference in D_b, but AF_p was higher for 1 % CLX gels ($p < 0.001$). A larger pore area would allow for oil to move through the network more easily, which in essence increasing the fraction of loosely oil bound (OL_1). However, CLX has shorter crystals compared to RBX ($p < 0.001$), corresponding to an increase in the fraction of tightly bound or adsorbed oil, resulting in less OL_4 for 1 % CLX gels.

OL_4 was higher for 1 % CLX gels compared to 1 % SFX gels ($p < 0.001$). There was no difference in D_b. However, 1 % CLX gels had a higher AF_p ($p < 0.01$) compared to 1 % SFX gels. OL_4 was higher for 2 % SFX gels compared to 2 % CLX gels ($p < 0.001$). Again, there was no difference in D_b, and 2 % SFX gels had a higher AF_p. In both cases, the gel with the higher AF_p retained less oil.

From this comparison, it is clear that under fast cooling conditions, 1 % SFX oleogels exhibited the highest oil

binding capacity. At higher wax concentrations, the oil binding capacity of RBX, SFX, and CLX oleogels were comparable and superior to the oil binding capacity of CS oleogels.

Conclusions

RBX, SFX, and CLX oleogels contained smaller crystals when cooled at 5 °C/min compared to 1 °C/min. In general, faster cooling decreased crystal size. For gels below 5 % wax concentration, this corresponded to an increase in D_b and a decrease in AF_p, creating a highly tortuous network with a higher oil binding capacity compared to slowly cooled gels. Under both cooling conditions, 1 % SFX gels exhibited superior oil binding capacity. At higher wax concentrations, SFX and CLX displayed similar oil binding capacities under slow cooling, while all three oleogels were comparable under fast cooling.

RBX consistently retained less oil than SFX, despite their similar morphology. This suggests that surface effects including surface chemistry and surface roughness should be examined as factors contributing to oil binding.

The oil binding capacity of CS oleogels was lower than that of wax oleogels at concentrations above 1 % (*w/w*). This suggests that the CS is a less efficient gelator since a greater concentration is required for gelation, and because CS oleogels retained less oil compared to wax oleogels. However, the oil binding capacity of CS oleogels can be improved by increasing the cooling rate.

Linear correlation analysis revealed that as AF_p increases, D_b decreases. A higher pore area fraction, or lower D_b, correlates with greater oil loss. In addition, oil loss increases with AF_p. The oil binding capacity of wax oleogels can be significantly improved if AF_p is decreased below 96 %.

Future work should evaluate the effect of shear on the microstructure and oil binding capacity of wax oleogels. In addition, the relationship between surface chemistry and surface texture and oil binding should be investigated. Such information will provide a better understanding of gelation mechanisms and the use of waxes as oil structuring materials.

Conflict of Interests There are no conflicts of interest.

References

1. R. Wang, X.-Y. Liu, J. Xiong, J. Li, J. Phys. Chem. B **110**, 7275 (2006)
2. M.A. Rogers, A.G. Marangoni, Cryst. Growth Des. **8**, 8 (2008)
3. A.G. Marangoni, D. Tang, A.P. Singh, Chem. Phys. Lett. **419**, 259 (2006)
4. M.A. Rogers, Soft Matter **4**, 1147 (2008)
5. N.K. Ojijo, I. Neeman, S. Eger, E. Shimoni, J. Sci. Food Agric. **84**, 1585 (2004)
6. S. Da Pieve, S. Calligaris, E. Co, M.C. Nicoli, A.G. Marangoni, Food Biophys. **5**, 211 (2010)
7. M.A. Rogers, A.G. Marangoni, Langmuir **25**, 8556 (2009)
8. E. Co, A.G. Marangoni, J. Am. Oil Chem. Soc. **90**, 529 (2013)
9. J.F. Toro-Vazquez, J.A. Morales-Rueda, E. Dibildox-Alvarado, M. Charó-Alonso, M. Alonzo-Macias, M.M. González-Chávez, J. Am. Oil Chem. Soc. **84**, 989 (2007)
10. J.A. Morales-Rueda, E. Dibildox-Alvarado, M.A. Charó-Alonso, R.G. Weiss, J.F. Toro-Vazquez, Eur. J. Lipid Sci. Technol. **111**, 207 (2009)
11. H.-S. Hwang, S. Kim, M. Singh, J.K. Winkler-Moser, S.X. Liu, J. Am. Oil Chem. Soc. **89**, 639 (2011)
12. D. Zulim Botega, Application of rice bran wax organogel to substitute solid fat and enhance unsaturated fat content in ice cream (Univeristy of Guelph, 2012), https://atrium.lib.uoguelph.ca/xmlui/handle/10214/3291 Accessed Jan 2015
13. A.J. Gravelle, S. Barbut, A.G. Marangoni, Food Funct. **4**, 153 (2013)
14. A.I. Blake, E.D. Co, A.G. Marangoni, J. Am. Oil Chem. Soc. **91**, 885 (2014)
15. A. Blake, A.G. Marangoni, Food Struct. **3**, 30 (2015)
16. K.J. Aryana, A.V.A. Resurreccion, M.S. Chinnan, L.R. Beuchat, J. Food Sci. **68**, 1301 (2003)
17. MIT Non-Newtonian Fluid Dynamics Research Group, http://web.mit.edu/nnf/education/wettability/wetting.html. Accessed 7 July 2015
18. A. Lafuma, D. Quere, Nat. Mater. **2**, 457 (2003)
19. M.S.G. Razul, C.J. MacDougall, C.B. Hanna, A.G. Marangoni, F. Peyronel, E. Papp-Szabo, D.A. Pink, Food Funct **5**, 2501 (2014)
20. A.G. Marangoni, Trends Food Sci. Technol. **13**, 37 (2002)
21. D. Tang, A.G. Marangoni, J. Am. Oil Chem. Soc. **83**, 377 (2006)